

# Glioma cancer stem cells induce immunosuppressive macrophages/microglia

Adam Wu, Jun Wei, Ling-Yuan Kong, Yongtao Wang, Waldemar Priebe, Wei Qiao, Raymond Sawaya, and Amy B. Heimberger

Department of Neurosurgery (A.W., J.W., L.-Y.K., Y.W., R.S., A.B.H.), Department of Experimental Therapeutics (W.P.), Department of Biostatistics (W.Q.), The University of Texas MD Anderson Cancer Center, Houston, Texas

Macrophages (MΦs)/microglia that constitute the dominant tumor-infiltrating immune cells in glioblastoma are recruited by tumor-secreted factors and are induced to become immunosuppressive and tumor supportive (M2). Glioma cancer stem cells (gCSCs) have been shown to suppress adaptive immunity, but their role in innate immunity with respect to the recruitment and polarization of MΦs/microglia is unknown. The innate immunosuppressive properties of the gCSCs were characterized based on elaborated MΦ inhibitory cytokine-1 (MIC-1), transforming growth factor (TGF-β1), soluble colony-stimulating factor (sCSF), recruitment of monocytes, inhibition of MΦ/microglia phagocytosis, induction of MΦ/microglia cytokine secretion, and the inhibition of T-cell proliferation. The role of the signal transducer and activator of transcription 3 (STAT3) in mediating innate immune suppression was evaluated in the context of the functional assays. The gCSCs produced sCSF-1, TGF-β1, and MIC-1, cytokines known to recruit and polarize the MΦs/microglia to become immunosuppressive. The gCSC-conditioned medium polarized the MΦ/microglia to an M2 phenotype, inhibited MΦ/microglia phagocytosis, induced the secretion of the immunosuppressive cytokines interleukin-10 (IL-10) and TGF-β1 by the MΦs/microglia, and enhanced the capacity of MΦs/microglia to inhibit T-cell proliferation. The inhibition of phagocytosis and the secretion of IL-10 were reversed when the STAT3 pathway was blocked in the gCSCs. The gCSCs modulate innate immunity in glioblastoma by inducing immunosuppressive MΦs/microglia, and this capacity can be reversed by inhibiting phosphorylated STAT3.

**Keywords:** cancer stem cells, innate immunity, macrophages, microglia, immune suppression, signal transducer and activator of transcription 3.

Glioblastoma multiforme (GBM) is a lethal cancer that responds poorly to radiotherapy and chemotherapy. Macrophages (MΦs) and microglia constitute the dominant tumor-infiltrating immune cells. MΦs/microglia that are capable of phagocytosis,<sup>1</sup> antigen processing and presentation,<sup>2</sup> cytotoxicity, and the promotion of inflammation<sup>3</sup> are designated M1. However, upon recruitment into the tumor microenvironment by chemoattractants such as CC chemokine ligand 2 (CCL2)<sup>4,5</sup> and soluble colony-stimulating factor 1 (sCSF-1),<sup>6,7</sup> MΦs/microglia become immunosuppressive<sup>8–10</sup> as designated as M2 and are unable to produce proinflammatory cytokines, induce effector T-cell energy, demonstrate impairments in cytotoxicity<sup>2,11–13</sup>, and induce Tregs.<sup>14</sup>

Tumor-associated MΦs are related to myeloid-derived suppressor cells, which have known immunosuppressive properties<sup>15</sup>; the tumor-associated MΦ probably represents a more mature subset of this cell population.<sup>16</sup> Tumor-associated M2 MΦs have been shown to promote cancer by secreting proangiogenic factors and enhancing invasion<sup>10,17</sup> mediated by the production of soluble factors such as transforming growth factor-β (TGF-β),<sup>18</sup> interleukin (IL)-1,<sup>19</sup> vascular endothelial growth factor, and matrix metalloproteinase-9.<sup>20</sup> The presence of MΦs correlates with poor prognosis in a variety of malignancies,<sup>21</sup> and polymorphism in the gene CX3CR1, which plays a role in MΦ and microglial mobilization and migration, was found to potentially be associated with differential survival in patients with GBM.<sup>22</sup> Thus, it appears that malignant gliomas actively recruit microglia and MΦs to the tumor site and induce them to adopt tumor-supportive phenotypes capable of mediating immunosuppression and promoting invasion. The mechanisms and participating cell populations that

Received February 18, 2010; accepted June 15, 2010.

Corresponding Author: Amy B. Heimberger, MD, Department of Neurosurgery, The University of Texas MD Anderson Cancer Center, 1515 Holcombe Blvd., Unit 442, Houston, TX 77030 (aheimber@mdanderson.org).

are mediating immunosuppressive MΦs/microglia have not been fully established.

Malignant gliomas contain glioma cancer stem cells (gCSCs) that are a heterogeneous population of multipotent undifferentiated cells with the capacity for self-renewal and are able to form neurospheres that are non-adherent *in vitro*, are highly tumorigenic,<sup>23</sup> and can recapitulate the characteristics of malignant gliomas.<sup>24</sup> We have recently shown that gCSCs are powerful mediators of immunosuppression of the adaptive immune system, specifically T-cell responses.<sup>25</sup> These processes are dependent on the phosphorylated signal transducer and activator of transcription 3 (p-STAT3) pathway,<sup>26</sup> which has been previously been demonstrated to be a key pathway in cancer-mediated immune suppression<sup>27</sup> and is overexpressed in most cancers including gliomas.<sup>28</sup>

STAT3 induces a variety of transcriptional factors that propagate tumorigenesis<sup>29</sup> and upregulate tumor-mediated immunosuppressive factors.<sup>27,30</sup> The STAT3-regulated tumor-secreted factors then activate STAT3 in diverse immune cells, including both innate immune cells such as MΦs and T cells,<sup>31</sup> resulting in global immune suppression.<sup>31–34</sup> When p-STAT3 is blocked in the gCSCs, cell proliferation is inhibited, neurosphere formation is impaired, the CD133-positive (CD133+) cells are depleted,<sup>35</sup> and the gCSC-mediated immunosuppression is blocked.<sup>26</sup> Additionally, using cytokine microarray analysis, we found that the gCSCs<sup>25</sup> were making MΦ inhibitory cytokine-1 (MIC-1), a member of the TGF-β super family,<sup>36</sup> which has been shown to be produced by glioblastoma cells<sup>37</sup> and found to be elevated in the cerebrospinal fluid of GBM patients, with higher levels associated with poorer outcome.<sup>38</sup> We have therefore hypothesized that the gCSCs can mediate innate immune suppression, possibly secondary to MIC-1, which can be reversed with STAT3 blockade. In this manuscript, we demonstrate that gCSCs induce MΦs derived from peripheral blood monocytes, the myeloid precursors to normal and tumor-infiltrating microglia/MΦs,<sup>39</sup> to an immunosuppressive phenotype that is partially reversed with STAT3 blockade.

## Material and Methods

### *Antibodies and Reagents*

Tissue culture grade monoclonal antibodies to CD3 (OKT3) and CD28 (28.6) were obtained from eBioscience. There are no commercially available specific inhibitors of MIC-1. WP1066 was synthesized and supplied by Waldemar Priebe and was stored as a 10-mM stock solution in dimethyl sulfoxide and diluted with phosphate-buffered saline (PBS) when used. Doses of 2 μM WP1066 were used, which is within the physiological dose range that can be achieved *in vivo*.<sup>40</sup> For flow cytometry, antibodies against CD11b and CD45 labeled with phycoerythrin (PE), fluorescein isothiocyanate (FITC), or allophycocyanin, and

corresponding IgG<sub>1</sub> isotypes were obtained from BD Pharmingen. CD133 antibody was obtained from Miltenyi Biotech, and p-STAT3 antibody and the corresponding IgG<sub>2</sub> isotypes were obtained from eBiosciences. ELISA kits for IL-10, TGF-β, sCSF-1, TNF-α, and MIC-1 were obtained from R&D Systems. ELISA antibodies for IL-23 were obtained from eBiosciences. Appropriate isotype controls were used for each antibody.

### *Human Tissues*

Tumor tissues from newly diagnosed GBM patients were obtained from surgery specimens and were graded pathologically according to the World Health Organization's classification system by a neuropathologist. Normal brain specimens were obtained from surgeries for extra-axial tumors (such as meningioma) where the surgical approach to access the tumor required the resection of a portion of overlying normal brain. All specimens were processed within 4 hours after resection. Each patient provided a written informed consent for tumor tissues, and this study was conducted under protocol #LAB03-0687, which was approved by the Institutional Review Board of The University of Texas MD Anderson Cancer Center.

### *Human gCSC Derivation*

The gCSCs were derived as described previously.<sup>41</sup> The gCSC may express CD133,<sup>42</sup> although this is not a definitive marker of stem cells.<sup>43–45</sup> There is no consensus on a definitive marker that can be used to determine "purity"; therefore, the characterization of the gCSC population was based on the criterion of *in vivo* tumorigenic potential, pluripotent potential, limiting dilution assays, and cytogenetic characterization,<sup>41</sup> which is consistent with our previously published reports.<sup>25,26</sup> After primary sphere formation was noted, sphere cells were dissociated for the characterization of the properties that distinguish gCSCs such as cell self-renewal, differentiation, and tumorigenesis. Supernatants from the gCSCs were collected and stored at -20°C for use as a conditioned medium and ELISA analysis. The frequency of occurrence of gCSCs isolated from GBM tumors was in the range 0.5%–10% based on the observed CD133 expression. Doubling time for the gCSCs was in the range of 2–4 days. Using limiting dilution analysis, neurosphere formation occurred at the following frequencies: 1 of 16 for gCSC1, which had 4% of cells expressing CD133+; 1 of 3 for gCSC2, which had 14% of cells expressing CD133+; 1 of 6 for gCSC3, which had 79% of cells expressing CD133+; and 1 of 9 for gCSC4, which had 21% of cells expressing CD133+. Neurospheres of similar size could be reformed after placing the parental neurosphere into single-cell suspension for at least 20 passages, demonstrating their self-renewal and proliferative properties. Cytogenetic testing of the neurospheres indicated that the gCSCs were of glioma tumor origin and not invading

neural progenitor cells based on the numerical and structural chromosomal aberrations of chromosomes 1 and 9. Furthermore, all 4 gCSCs expressed the repressor element 1-silencing transcription factor (REST).<sup>46</sup> The gCSCs were cultured *in vitro* with the neurosphere medium consisting of Dulbecco's modified Eagle's medium/F-12 medium containing 20 ng/mL of both epidermal growth factor and fibroblast growth factor 2.

#### *CD133 Depletion of Bulk GBM*

Single-cell suspensions of fresh primary GBM surgical specimens were prepared by mechanical dissociation and digestion with a type I collagenase (Sigma) for 1 hour at 37°C. Cells were isolated on a 44%/66% Percoll gradient, and CD133+ cells were depleted by magnetic separation using CD133 microbeads as per the manufacturer's instructions (Miltenyi Biotec). CD133 depletion was verified by flow cytometry. Bulk and CD133-depleted tumor cells were cultured at  $1 \times 10^6$  cells/mL in the neurosphere medium for 72 hours in a humidified atmosphere of 95% air/5% CO<sub>2</sub> before supernatants were collected for use as experimental controls.

#### *Human Peripheral Blood Mononuclear Cells and Differentiation of Monocyte-Derived MΦs*

Peripheral blood mononuclear cells (PBMCs) were prepared from healthy donor blood (Gulf Coast Blood Center) by centrifugation on a Ficoll-Hypaque density gradient (Sigma-Aldrich). Monocytes were purified using CD14 microbeads according to the manufacturer's directions (Miltenyi Biotec). Monocytes were cultured for 5 days in the RPMI 1640 medium supplemented with 10% fetal bovine serum (FBS) and 50 U/mL granulocyte-macrophage colony-stimulating factor (GM-CSF; eBiosciences) in order to induce differentiation into MΦs<sup>47</sup> at 37°C in a humidified atmosphere of 95% air/5% CO<sub>2</sub>.

#### *Isolation and Culture of Microglia*

Microglia, the predominant immune cells in the CNS,<sup>17,48</sup> are MΦs.<sup>49</sup> Although murine microglia can be distinguished from MΦs based on CD45 expression,<sup>50</sup> in humans the distinction is far more ambiguous, and to date, no single histological marker has been described that can reliably distinguish microglia from MΦs in human gliomas. Thus, these cells were purified using a Percoll gradient as we have described previously.<sup>12</sup> The microglia/MΦs were collected from the 1.03 (g/mL)/1.065 (g/mL) and 1.065 (g/mL)/1.072 (g/mL) Percoll density layer interfaces, and their purity was ascertained using flow cytometry for the detection of CD45 and CD11b. Purified microglia/MΦs were cultured in the RPMI 1640 medium supplemented with 10% FBS and 50 U/mL GM-CSF for 24–48 hours prior to further experimentation.

#### *Treatment of MΦs with Medium Conditioned by gCSCs*

Normal microglia or MΦs were each cultured for 48 hours in a medium previously conditioned by bulk GBM supernatants in the neurosphere medium, bulk GBM supernatants with CD133+ depletion in the neurosphere medium, gCSCs, neurosphere medium, or neurosphere media with the addition of MIC-1. Cells were harvested, and surface marker expression was analyzed by flow cytometry. The culture supernatant was collected and analyzed with ELISA.

#### *Flow Cytometry*

Purity of the MΦs and microglia after isolation was tested using FITC-conjugated anti-CD45 and PE-conjugated anti-CD11b, whereas the intracellular staining of p-STAT3 was done using PE-conjugated anti-p-STAT3, along with the corresponding IgG<sub>1</sub> or IgG<sub>2</sub> isotypes. Flow cytometry acquisition was done with a FACSCaliber (Becton Dickinson), and data analysis was performed using FlowJo software (TreeStar). Live cells were gated using forward and side scatters, and positive staining was determined using a threshold of >1% on the isotype sample.

#### *ELISA Measurement of Cytokines in Medium Conditioned by gCSCs*

The supernatant medium conditioned by gCSCs was measured for cytokine concentrations using ELISA kits as described (R&D Systems). The supernatants were collected after 5 days in culture and stored at –20°C. For ELISA tests, the supernatants were added in duplicate to appropriate coated plates. After the plates were washed, horseradish peroxidase-conjugated detection antibody was added. The substrate used for color development was tetramethylbenzidine. The optical density was measured at 450 nm with a microplate reader (Spectra Max 190; Molecular Devices), and chemokine concentrations were quantified with SoftMax Pro software (Molecular Devices). The detection limits for sCSF-1 were 16 pg/mL; for MIC-1, 8 pg/ml; for TNF-α, 31 pg/mL; for IL-23, 31 pg/mL; for IL-10, 16 pg/mL; and for TGF-β1, 31 pg/mL.

#### *Cell Migration Assay*

Cell migration assay kits (Cell Biolabs) were obtained and migration assays conducted as per the manufacturer's instructions. The culture well inserts (provided with a membrane pore size of 5 μM) were seeded with CD14+ human monocytes and placed in 24-well culture plates containing either neurosphere medium (as the negative control), bulk GBM supernatants in neurosphere medium, bulk GBM supernatants with CD133 depletion in neurosphere medium, gCSC-conditioned medium, or a medium containing 10 ng/mL sCSF-1 (positive control). After overnight culture, all the cells that migrated through the membrane into the

experimental medium were collected, pelleted with centrifugation, resuspended in a unit volume, and manually counted using a hemocytometer. Total migration was calculated as a percentage of the negative control.

#### T-Cell Proliferation Assay

T-cell proliferation was determined using a carboxyfluorescein diacetate succinimidyl ester (CFSE)-based assay,<sup>51</sup> which we have used previously.<sup>12,25,26,40</sup> In brief, healthy donor PBMCs were labeled with 2  $\mu$ M CFSE for 5 minutes at room temperature in PBS, and then the reaction was quenched with the RPMI 1640 medium with 10% FBS for 10 minutes at 37°C. The 48-well culture plates were incubated with 1  $\mu$ g/mL anti-CD3/anti-CD28 in PBS for 1 hour. About  $2 \times 10^5$  PBMCs/well were plated in the 48-well plates with pre-bound anti-CD3/anti-CD28, and the conditioned medium from gCSCs and M $\Phi$ s was added to the stimulated PBMCs. The cells were harvested for analysis after 96 hours.

#### Phagocytosis Assay

After incubation for 48 hours with experimental supernatants as described above, the microglia or M $\Phi$  cell viability was assessed by Trypan Blue exclusion, and live microglia or M $\Phi$ s were transferred to a 96-well plate at a concentration of  $1.0 \times 10^5$  cells/well and incubated at 37°C in a humidified atmosphere containing 95% air/5% CO<sub>2</sub> for 1 hour to allow the cells to adhere. The cells were then incubated with pHrodo *Escherichia coli* BioParticles (Invitrogen) suspended in PBS for 2 hours at 37°C at atmospheric CO<sub>2</sub> levels. The supernatant containing the bioparticles was then removed and the cells incubated for 15 minutes with DAPI (Vector Laboratories) at room temperature in order to identify the nuclei. In order to quantify phagocytosis, digital images were taken using fluorescence microscopy ( $\times 20$  magnification) under identical camera exposure and compensation settings for control and experimental conditions. Each image was analyzed using Adobe Photoshop CS software. Background fluorescence in the cell-free regions for each image was determined. The fluorescence intensity in each individual cell was then measured and corrected for the background. The overall level of phagocytosis was expressed as mean fluorescence intensity per cell. Percent phagocytosis levels relative to the control (neurosphere medium alone) were calculated for each experimental condition.

#### STAT3 siRNA Transfection

To knockdown STAT3 gene expression, STAT3 small interfering RNA (siRNA) was transfected into gCSC lines as described by the manufacturer (Santa Cruz Biotech). Briefly,  $0.5 \times 10^6$  gCSCs per well were seeded in a 6-well plate. siRNA duplex solution (1  $\mu$ g STAT3 siRNA or 2 controls of siRNA A and B) in 100  $\mu$ L of siRNA transfection medium was prepared and gently mixed with siRNA transfection reagent in

100  $\mu$ L of siRNA transfection medium, incubated for 45 minutes at room temperature, and then diluted to a final volume of 1 mL and overlaid on the cells. The cells were incubated for 5 hours at 37°C, followed by the addition of 1 mL of the neurosphere medium and incubation overnight. The medium was then replaced with a fresh neurosphere medium, and the cells were incubated for an additional 48 hours.

#### pSTAT1 Western Blot

After exposure to the gCSC-conditioned medium and other experimental conditions for 48 hours, the M $\Phi$ s were harvested, pelleted by centrifugation, and rinsed with ice-cold PBS at 380 g for 5 minutes. The cells were lysed for 30 minutes in an ice-cold lysis buffer (50 mM Tris-HCl [pH 8.0], 150 mM NaCl, 1 mM EDTA) containing 1% Triton X-100 and phosphatase and protease inhibitors (Sigma-Aldrich). The lysates were centrifuged at 14 000 rpm for 10 minutes at 4°C. The supernatants were collected and quantified for the protein content. Equal amounts of proteins (20  $\mu$ g) were electrophoretically fractionated in 8% sodium dodecyl sulfate-polyacrylamide gels, transferred to nitrocellulose membranes, and subjected to immunoblot analysis with specific antibodies against p-STAT1 (Tyr701; Cell Signaling Technology, Inc.). Autoradiography of the membranes was performed using Amersham ECL Western-blotting detection reagents (Amersham Biosciences).

#### Statistical Analysis

The distribution of each continuous variable was summarized by its mean, standard deviation, and range. The Wilcoxon rank-sum test was conducted for the comparison of any 2 groups. The corresponding non-parametric sign-rank test for paired *t*-test was used to compare experimental and control groups that were matched. Owing to the exploration nature of this study, type I error was not adjusted in cases of multiple comparisons. All computations were carried out in SAS version 9.1. Error bars represent the standard deviation.

## Results

#### gCSCs Secrete Cytokines that Regulate Innate Immunity

We have previously isolated gCSCs at the time of surgery from patients newly diagnosed with GBM and shown that these cells form neurospheres, are capable of multipotential differentiation, and can induce tumors at low doses.<sup>25</sup> The gCSCs ( $n = 4$ ) produced TGF- $\beta$ 1 (range: 8.7–133.9 pg/10<sup>6</sup> cells/24 h), MIC-1 (range: 22.3–1056.2 pg/10<sup>6</sup> cells/24 h), and sCSF-1 (range: 6.3–38.8 pg/10<sup>6</sup> cells/24 h), but not TNF- $\alpha$  or IL-10 (Table 1).

**Table 1.** Production of cytokines that influence innate immunity by gCSC lines

gCSC	Cytokine production <sup>a</sup> (pg/mL/10 <sup>6</sup> cells/24 h)		
	MIC-1	CSF-1	TGF-β1
1			
Range	402.0–1773.1	1.6–89.3	56.8–193.4
<i>n</i>	4	3	3
Mean ± SD	1056.2 ± 687.7	55.7 ± 47.3	133.9 ± 70.0
2			
Range	108.9–366.5	0.6–67.3	18.8–62.0
<i>n</i>	4	3	4
Mean ± SD	228.4 ± 129.8	31.6 ± 33.6	35.8 ± 20.0
3			
Range	0–94.1	0–12.6	1.3–26.9
<i>n</i>	4	3	3
Mean ± SD	22.3 ± 19.5	5.7 ± 6.4	16.1 ± 13.3
4			
Range	4734–1183.6	0.3–27.6	0–23.5
<i>n</i>	4	3	3
Mean ± SD	898.4 ± 368.1	13.9 ± 13.6	8.7 ± 12.8

MIC-1, Macrophage inhibitory cytokine-1; CSF-1, Colony-stimulating factor-1; TGF-β1, Transforming growth factor-β1; SD, Standard deviation.

<sup>a</sup>Detection limit for ELISA is 0.015 ng/mL (0.6 pg/mL/10<sup>6</sup> cells/24 h for 5 × 10<sup>6</sup> cells cultured for 5 days).

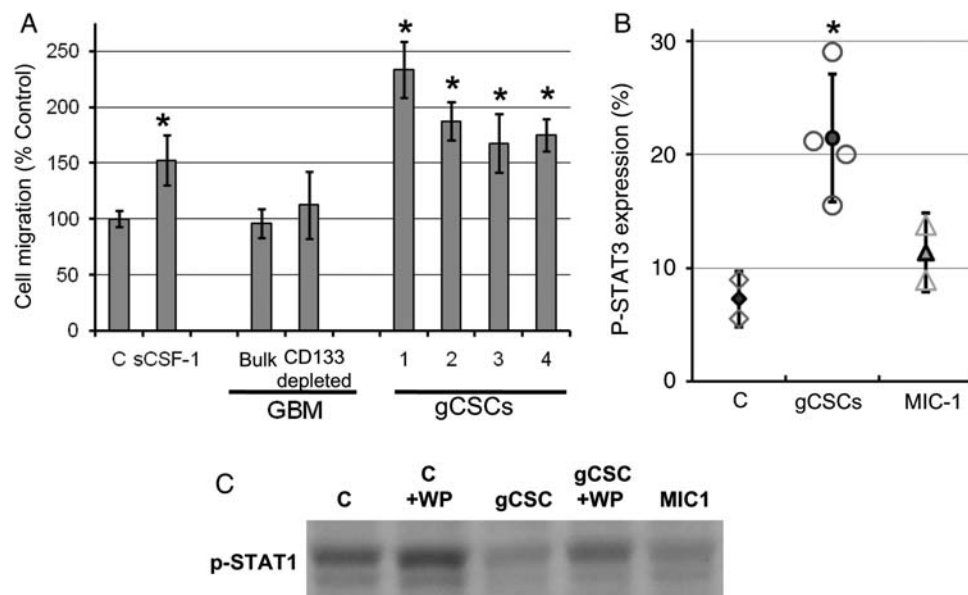


**Fig. 1.** Attraction and phenotype alteration of monocytes by gCSCs. Monocytes upon exposure to the gCSC-conditioned medium ( $n = 4$ ) demonstrated (A) increased migration in a cell-migration chemotaxis assay compared with both control neurosphere medium alone and supernatants from bulk and CD133<sup>+</sup> depleted primary GBM and (B) an increase in p-STAT3 expression, as shown by flow cytometry, relative to control monocytes exposed to neurosphere medium alone. (C) Western blot showing that p-STAT1 expression was decreased within monocytes and MΦs by gCSC-conditioned medium and MIC-1, and that this was partially reversed by p-STAT3 blockade with WP1066 (WP = 2 μM WP1066). C is control neurosphere medium.

### gCSCs Induce Migration of Monocytes

To ascertain whether the gCSCs can induce migration of the monocytes, the medium conditioned by single-cell suspensions from newly diagnosed GBM, single-cell suspensions from newly diagnosed GBM depleted of

CD133<sup>+</sup> cells, and the gCSCs were tested in a cell migration chemotaxis assay (Fig. 1A). All four gCSCs potentially induced migration (range, 168 ± 26%–362 ± 33% relative to controls;  $P = .03$ ) of the monocytes in a manner similar to our positive control medium containing sCSF-1 (152 ± 23%–261 ± 27%

relative to control;  $P = .03$ ), a known chemoattractant for monocytes. The amount of sCSF-1 produced by each gCSC line correlated in a nonlinear fashion with the degree of monocyte migration induced. Whereas the single-cell suspensions from the newly diagnosed GBM patients, including those depleted of CD133+ cells, failed to significantly induce migration of monocytes in comparison to the control neurosphere medium.

#### gCSCs Induce p-STAT3 Expression in Monocytes

When monocytes were cultured in the gCSC-conditioned medium, the morphology of the monocytes changed to become flattened, adherent, and irregularly shaped, with cell processes that were consistent with MΦ morphology. Incubation of the monocytes for 24 hours with the conditioned medium from each of the respective gCSC lines ( $n = 4$ ) markedly induced an increase in the expression of p-STAT3 (Fig. 1B) relative to control monocytes ( $n = 2$ ) incubated in the neurosphere medium alone (range: 15.5%–29.0%; mean  $21.4 \pm 5.6\%$ , compared with 5.5%–9.0%; mean  $7.3 \pm 2.4\%$ ).

#### gCSCs Down Modulate p-STAT1 Expression in MΦs

Proinflammatory M1 MΦs express p-STAT1, and upon polarization toward an immunosuppressive phenotype

(M2), show a decrease in the expression of p-STAT1 with a relative increase in the expression of p-STAT3.<sup>52</sup> Therefore, we assessed the expression of p-STAT1 in MΦs after exposure to the gCSC-conditioned medium. The gCSC supernatants down modulated the expression of p-STAT1 in MΦs relative to controls treated with the neurosphere medium alone, and this down modulation was partly reversed if the MΦs were also treated with WP1066 (Fig. 1C).

#### gCSCs Inhibit MΦ and Microglia Phagocytosis

To evaluate the role of gCSCs on MΦ function, human monocytes were isolated from peripheral blood of normal donors and induced to differentiate into MΦs in vitro.<sup>47</sup> Phenotypic markers indicated at least >95% purity based on the CD14<sup>+</sup>CD45<sup>+</sup>CD11b<sup>+</sup> expression observed. The medium cultured by all of the gCSC supernatants inhibited phagocytosis by the MΦs (representative example shown in Fig. 2A,i and ii; gCSC1,  $59.9\% \pm 2.2\%$  of neurosphere medium alone,  $P = .05$ ,  $n = 3$ ; gCSC2,  $44.9\% \pm 4.5\%$ ,  $P = .03$ ,  $n = 4$ ; gCSC3,  $58.6\% \pm 17.4\%$ ,  $P = .03$ ,  $n = 4$ ; gCSC4,  $63.7\% \pm 19.1\%$ ,  $P = .03$ ,  $n = 4$ ). Whereas bulk primary GBM supernatant ( $104.5\% \pm 2.5\%$ ,  $P = .31$ , Fig. 2A,iii) and CD133+ depleted primary

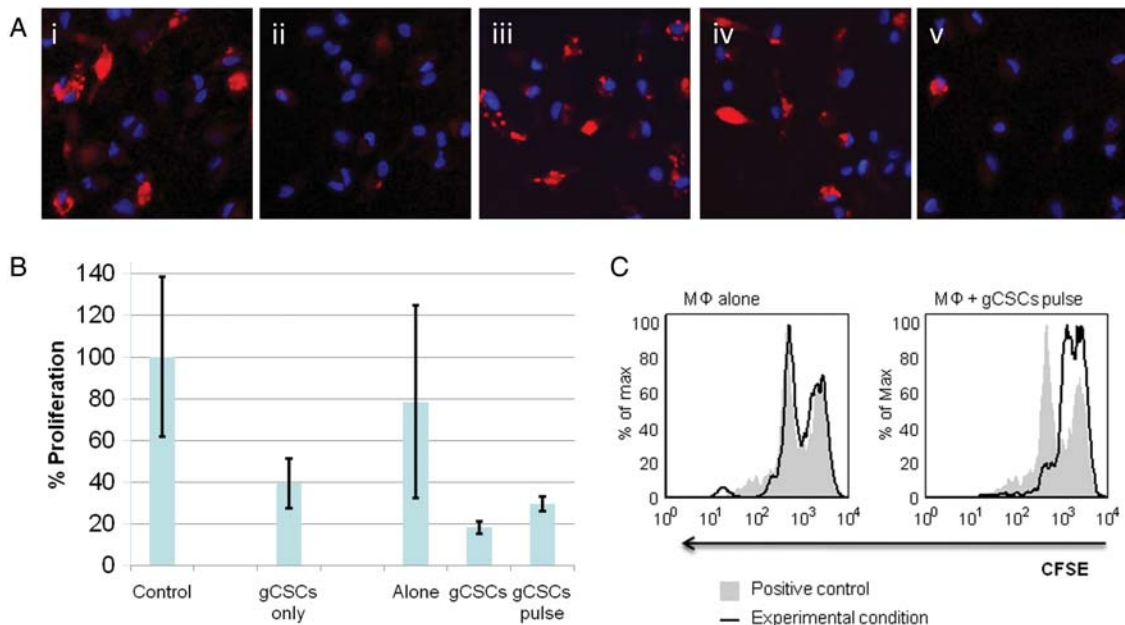


Fig. 2. Functional inhibition of MΦs/microglia by gCSCs. (A) Representative microscope ( $\times 40$ ) images showing inhibition of phagocytosis of fluorescent microbeads (red) in MΦs exposed to (i) positive control (neurosphere medium) compared with (ii) gCSC-conditioned medium. In contrast, (iii) bulk primary GBM supernatant and (iv) CD133+ depleted primary GBM supernatant did not inhibit phagocytosis. Furthermore, representative microscopy demonstrates that phagocytosis is inhibited in MΦs exposed to (v) 10 ng/mL MIC-1. MΦ nuclei were stained with DAPI (blue). A similar inhibition of phagocytosis by the gCSC-conditioned medium was seen in normal microglia (Supplementary Fig. 1). (B) T-cell proliferation was inhibited by MΦs treated with gCSC-conditioned medium ( $n = 4$ ) compared with MΦs treated with neurosphere medium alone. When MΦs were pulsed with gCSC-conditioned medium ( $n = 4$ ), inhibition of T-cell proliferation was maintained even after gCSC-conditioned medium was removed and replaced with a fresh growth medium. Inhibition of T-cell proliferation is expressed as a percent positive control neurosphere medium alone (\*significantly different from MΦs alone;  $P < .05$ ). (C) Representative CFSE histograms comparing the inhibition of T-cell proliferation between MΦs alone and MΦs pulsed with the gCSC-conditioned medium.

GBM (99.2% ± 4.5% of neurosphere medium alone, Fig. 2A,iv) had no appreciable effect. The degree of phagocytosis inhibition did not correlate with CD133 expression. Similar results were found with human microglia in which the gCSCs inhibited phagocytosis to 57%–62% ( $n = 2$ ) in comparison to the neurosphere medium alone (Supplementary Fig. S1).

#### gCSCs Induce MΦs to Produce Immunosuppressive Cytokines

To ascertain if the gCSCs were triggering the production of known MΦ-elaborated immunosuppressive cytokines such as TGF-β1,<sup>14</sup> IL-10,<sup>53</sup> and IL-23,<sup>54</sup> the MΦs were treated with a medium conditioned by the gCSCs and compared with control MΦs treated with the neurosphere medium alone. The control MΦs ( $n = 3$ ) elaborated TGF-β1 (range: 200–1280 pg/10<sup>6</sup> cells/24 h) and IL-10 (range: 40–280 pg/10<sup>6</sup> cells/24 h) but not IL-23. IL-10 production was enhanced by a medium conditioned by all of the gCSC lines (Table 2) (range: 310–11 880 pg/10<sup>6</sup> cells/24 h; range: 1.1–23.1-fold increase relative to control;  $n = 4$ ). Furthermore, either

TGF-β1 production (range: 310–4280 pg/10<sup>6</sup> cells/24 h; range: 0.8–4.6-fold increase relative to control) or IL-23 was induced (range: 180–5650 pg/10<sup>6</sup> cells/24 h) by the gCSC lines ( $n = 4$ ) (Table 2). Similarly, the gCSCs also induced IL-23 (range: 0–403.6 pg/10<sup>6</sup> cells/24 h) and enhanced TGF-β1 secretion (from 1158.6 pg/10<sup>6</sup> cells/24 hours to between 1331.8 and 1475.3 pg/10<sup>6</sup> cells/24 h, a 1.1–1.3-fold increase) in normal human microglia ( $n = 2$ ).

#### gCSCs Potentiate MΦ and Microglia Inhibition of T-cell Proliferation

Because the gCSCs induce the MΦs to increase the production of immunosuppressive cytokines, we next wanted to ascertain whether these cytokines were functionally active as determined by their ability to inhibit T-cell proliferation. Exposure of the MΦs to the gCSC-conditioned medium ( $n = 4$ ) significantly increased the ability of the medium conditioned by MΦs and microglia to inhibit T-cell proliferation by 68.0%–77.5% ( $P = .03$ ) relative to the culture medium from MΦs treated with a control neurosphere

**Table 2.** Induction of cytokine secretion in MΦs exposed to the conditioned medium from gCSCs

gCSC	MΦs	IL-10 (pg/mL/10 <sup>6</sup> cells/24 h in culture)			TGF-β1 (pg/mL/10 <sup>6</sup> cells/24 h in culture)			IL-23-conditioned medium <sup>b</sup> (pg/mL/10 <sup>6</sup> cells/24 h in culture)
		Control medium	Conditioned medium	X-fold <sup>a</sup> control	Control medium	Conditioned medium	X-fold control	
gCSC1	1	50 ± 0	360 ± 20	6.8	1280 ± 80	3220 ± 1010	2.5	0
	2	30 ± 0	150 ± 10	5.3	200 ± 0	310 ± 100	1.5	0
	3	110 ± 10	200 ± 15	1.9	420 ± 30	360 ± 40	0.8	0
	Mean	60 ± 40	240 ± 110	4.7 ± 2.5	640 ± 570	1300 ± 1670	1.6 ± 0.8	0
gCSC2	1	110 ± 10	240 ± 70	2.2	1280 ± 80	4280 ± 80	3.3	0
	2	50 ± 0	220 ± 30	4	203 ± 0	930 ± 10	4.6	0
	3	30 ± 0	120 ± 10	4.1	420 ± 30	700 ± 80	1.7	0
	4				790 ± 80	1530 ± 160	1.9	
Mean	60 ± 40	190 ± 60	3.5 ± 1.1	670 ± 470	1860 ± 1650	2.9 ± 1.4	0	
gCSC3	1	110 ± 10	430 ± 420	4	1280 ± 80	1300 ± 920	1	1660
	2	510 ± 130	11 890 ± 1320	23.1	200 ± 0	250 ± 0	1.2	330
	3	50 ± 0	140 ± 20	2.6	450 ± 240	350 ± 0	0.8	4030
	Mean	220 ± 250	4030 ± 6800	9.9 ± 11.5	640 ± 560	630 ± 580	1.0 ± 0.2	2000 ± 1870
gCSC4	1	110 ± 10	460 ± 90	4.3	1280 ± 80	360 ± 30	0.3	3880
	2	40 ± 0	650 ± 320	16.3	200 ± 0	100 ± 20	0.5	5650
	3	50 ± 0	60 ± 0	1.1	420 ± 30	450 ± 10	1.3	600
	Mean	70 ± 30	390 ± 300	7.2 ± 8.0	640 ± 570	300 ± 180	0.7 ± 0.5	3380 ± 2560
MIC-1 ng/mL	1	510 ± 130	500 ± 480	1	420 ± 30	520 ± 40	1.2	0
	2	40 ± 0	50 ± 10	1.3	450 ± 240	570 ± 60	1.3	0
	Mean	280 ± 340	280 ± 320	1.1 ± 0.2	430 ± 20	540 ± 30	1.2 ± 0.0	0
MIC-10 ng/mL	1	50 ± 0	110 ± 10	2	420 ± 30	580 ± 80	1.4	0
	2	30 ± 0	80 ± 10	3	60 ± 10	400 ± 140	6.9	0
	3	60 ± 0	290 ± 20	4.6	790 ± 80	880 ± 180	1.1	0
	Mean	50 ± 20	160 ± 110	3.2 ± 1.3	430 ± 370	620 ± 240	3.1 ± 3.2	0

MΦ, macrophages; IL, interleukin; TGF-β1, transforming growth factor-β1; MIC-1, macrophage inhibitory cytokine-1.

<sup>a</sup>Number of times (fold) the level seen in the control.

<sup>b</sup>Control macrophages produced no IL-23.

medium, which did not significantly affect the T-cell proliferation (Fig. 2B and C). Because the gCSC-conditioned medium alone can inhibit T-cell proliferation (range: 43.5%–70.3% of the neurosphere medium alone), to confirm that the gCSC-conditioned MΦs were contributing to the inhibition of T-cell proliferation, the MΦs were washed and the medium was replaced after the MΦs were exposed to the gCSC-conditioned medium. The supernatant medium from these gCSC-pulsed MΦs retained the ability to inhibit T-cell proliferation (range: 48.5%–57.3% relative to MΦs treated with the control neurosphere medium,  $P = .03$ ) even in the absence of any factors directly produced by gCSCs. Similarly, the medium conditioned by normal microglia without exposure to the gCSC-conditioned medium did not significantly inhibit T-cell proliferation but did inhibit T-cell proliferation by 75.2%–75.5% ( $n = 2$ ) after exposure to the gCSC-conditioned medium.

#### *The Immunosuppressive Role of the p-STAT3 Pathway in gCSC-Mediated MΦ Immunosuppression*

To determine if p-STAT3 blockade can change the innate immunosuppressive functions of the gCSCs, the gCSCs were treated with either the STAT3 siRNA or the small molecule inhibitor WP1066 at levels that do not affect cell viability.<sup>26</sup> The induction of IL-10 production in MΦs by the gCSC-conditioned medium was reduced when p-STAT3 was inhibited in gCSCs by WP1066 ( $0.5 \pm 0.1$ -fold control) and STAT3 siRNA ( $0.7 \pm 0.1$ -fold control) compared with untreated gCSCs ( $1.7 \pm 0.1$ -fold control) but not by either of the 2 control siRNAs ( $2.5 \pm 0.2$ -fold and  $3.8 \pm 0.1$ -fold control, respectively; Fig. 3A). In contrast, IL-23 and TGF- $\beta$ 1 induction in the MΦs was not decreased to a statistically significant degree when p-STAT3 was inhibited in gCSCs (data not shown).

To determine if the inhibition of phagocytosis by gCSCs is mediated by the p-STAT3 pathway, 2 gCSC lines were treated with WP1066 and siRNA, and MΦs were exposed to the resulting conditioned medium (Fig. 3B). For both gCSC lines, the inhibition of phagocytosis by the gCSCs (range: 44.9%–67.7%) was reversed by both WP1066 (range: 75.1%–110.6%) and STAT3 siRNA (range: 95.2%–100.2%) but not by either of the two different control siRNAs (ranges: 16.9%–57.8% and 44.2%–66.8%, respectively).

#### *The Role of gCSC MIC-1 in Immunosuppressive MΦs*

As described above, we found that gCSCs produced MIC-1 at a physiological range of 0.16–47.7 ng/mL and therefore evaluated the role that MIC-1 played in the ability of gCSCs to induce immunosuppressive MΦs, by treating monocytes and MΦs with the neurosphere medium containing MIC-1 at doses within this physiological range. At a dose of 10 ng/mL ( $n = 2$ ), MIC-1 had no effect on the expression of cell surface markers by monocytes (data not shown) but did

marginally increase the expression of p-STAT3 (range: 8.9%–13.8%; mean  $11.4 \pm 3.5\%$  relative to the neurosphere medium control; Fig. 1C). MIC-1 also decreased the expression of p-STAT1 in MΦs (Fig. 1D). Exposure of either the MΦs or microglia to MIC-1 resulted in a marked inhibition of phagocytosis ( $62.8\% \pm 7.3\%$ ,  $P = .05$ ,  $n = 3$ ; Fig. 2B,v). Secretion of both TGF- $\beta$ 1 and IL-10 (but not of IL-23) was increased by MIC-1 (Table 2) but generally to a degree less than that observed for the gCSC-conditioned medium. STAT3 blockade in the gCSCs also did not significantly reduce their production of MIC-1 (data not shown), suggesting that gCSCs may be able to induce immunosuppressive MΦs/microglia via multiple pathways, some of which may be independent of gCSC p-STAT3 pathways.

## Discussion

In this report, we demonstrate that the gCSCs contribute to the conversion of monocytes to an immunosuppressive MΦ/microglia (M2) phenotype by a variety of secreted factors. Previously, both glioma-elaborated CCL2 and sCSF-1 had been shown to recruit monocytes into the tumor microenvironment. Our ELISA data demonstrate that the gCSCs secrete these factors and that the gCSC-conditioned medium increases monocyte migration, indicating that the gCSCs are probably recruiting monocytes into the tumor microenvironment. Supportive of this contention is that the single-cell suspensions from the GBM, which contain a low frequency of gCSCs (1%–3% CD133<sup>+</sup> cells), as anticipated, failed to significantly induce the migration of monocytes. We have also provided several pieces of evidence indicating that the gCSC is then polarizing the MΦ/microglia toward the immunosuppressive (M2) phenotype. First, based on Western blot analysis and intracellular cytokine staining, the gCSCs down modulated p-STAT1 and upregulated p-STAT3 within the monocyte population. These data are consistent with a previous report demonstrating upregulation of p-STAT3 in dendritic cells.<sup>31</sup> Furthermore, we demonstrated that the gCSC induces the MΦ to produce immunosuppressive cytokines that functionally inhibit T-cell proliferation and effector responses.

We also showed that gCSCs impede the phagocytosis ability of MΦs/microglia. A reduction in phagocytic capacity does not necessarily imply an immunosuppressive phenotype, as M2 MΦs can in some circumstances efficiently phagocytose,<sup>55</sup> which is not surprising given the normal physiological role of M2 MΦs in debris scavenging.<sup>56</sup> Rather, the in vitro inhibition of phagocytosis of microbeads we demonstrate here may represent a direct suppression of M1 effector function, which may or may not be independent of a concurrent polarization toward the M2 phenotype. Thus, in addition to the inhibition of adaptive immune responses that we have shown previously,<sup>25,26</sup> we find that gCSCs are additionally exerting immunosuppression of the innate immune system—the first report to date to our knowledge.



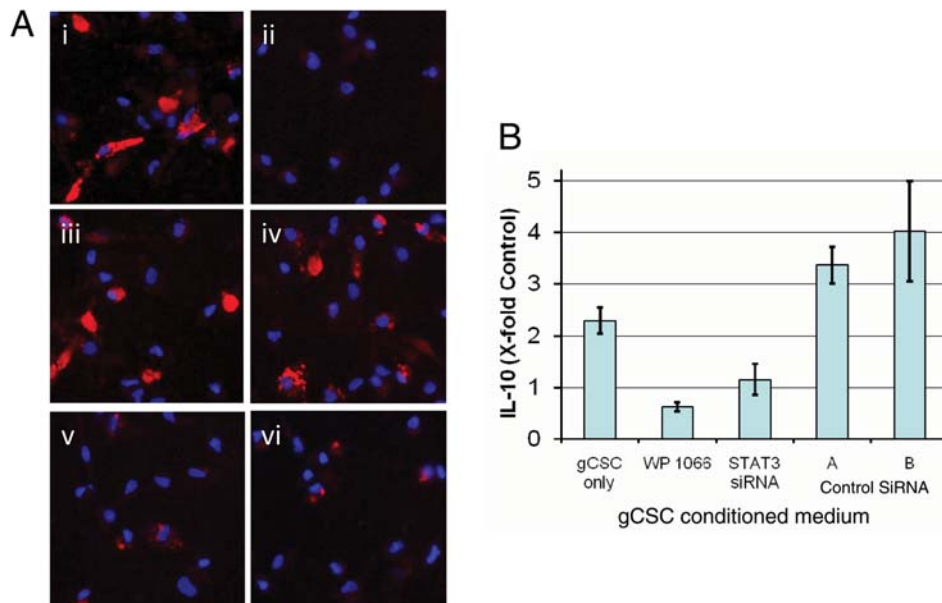


Fig. 3. STAT3 blockade diminishes gCSC-mediated modulation of MΦ immunosuppressive function. (A) Representative microscope ( $\times 40$ ) images showing phagocytosis in MΦs exposed to (i) control medium and (ii) gCSC-conditioned medium ( $67.7\% \pm 4.3\%$  of control level), with reversal of phagocytosis inhibition after inhibition of STAT3 in gCSCs by (iii)  $2 \mu\text{M}$  WP1066 medium ( $110.6\% \pm 15.8\%$  of control level), and (iv) STAT3 siRNA ( $100.2\% \pm 5.8\%$  of control level), but not by 2 different control siRNAs, (v)  $57.8\% \pm 3.5\%$  of control level and (vi)  $66.8\% \pm 1.3\%$  of control level, respectively. MΦ nuclei stained with DAPI. (B) STAT3 blockade reversed the induction of MΦ IL-10 production by gCSCs. The increase in MΦ IL-10 production by the gCSC-conditioned medium was reduced by treatment of gCSCs with WP1066 and STAT3 siRNA to levels not significantly different from that of controls treated with the neurosphere medium, whereas MΦ IL-10 production induced by gCSCs treated with 2 different control siRNAs remained significantly increased relative to controls treated with the neurosphere medium.

The gCSC induction of immunosuppressive cytokines by MΦs was variable. For example, some gCSCs increased TGF- $\beta 1$ , whereas others induced IL-23. The magnitude of cytokine production also varied between MΦs derived from different donors and as a result the increases in cytokine production did not reach statistical significance. However, in nearly all instances where a particular gCSC increased the production of a particular cytokine, an increase was seen with every donor MΦ tested supporting the contention of the gCSCs triggering MΦ elaborated immune suppressive cytokines. There is also the possibility, as some production of both IL-10 and TGF- $\beta 1$  was observed consistently in control MΦs, that constitutive immunosuppressive cytokine production by MΦs may be more important in vivo than any further induced increases, with the recruitment of the MΦs being the more important role of the gCSCs. However, we did find that supernatants conditioned by MΦs exposed to gCSCs inhibited T-cell proliferation to a greater extent than MΦs alone, which suggests that increases in MΦ cytokine production mediated directly by gCSCs does have physiological consequences.

Extrapolating the rates of cytokine production measured in vitro to in vivo cytokine levels is challenging since in vivo levels will be dependent on multiple factors, including cell densities, proximity of various cell types to one another, rates of efflux and elimination, multiple sources of production, and local environmental factors such as hypoxia to name a few. This caveat also

applies to the physiological significance of the phagocytosis and T-cell proliferation inhibition. For example, serum levels of TGF- $\beta 1$  in human GBM patients have been reported to be approximately  $800 \text{ pg/mL}$ <sup>57</sup> and murine intratumoral TGF- $\beta 1$  levels to be around  $60 \text{ pg/mg}$  of total protein that correlated with a 2-fold increase in FoxP3+ Treg infiltration<sup>58</sup>. In terms of functionally relevant in vivo changes in cytokine levels, treatment that resulted in a significant inhibition of tumor growth in an animal model of lung cancer resulted in a 2-fold decrease in the intratumoral concentrations of both IL-10 and TGF- $\beta 1$ .<sup>59</sup> Given the paucity of correlative in vivo intratumoral data, the physiological relevance of changes in the various cytokines we observed in vitro is therefore indeterminate.

On the basis of the cytokine microarray data, we noted that the gCSCs produced abundant MIC-1 that was lost upon differentiation.<sup>25</sup> Furthermore, other studies have shown that MIC-1 is an inducer of STAT3 in neurons<sup>60</sup> and that MIC-1 exerts immunosuppressive effects on MΦs.<sup>36</sup> We therefore investigated whether MIC-1 was specifically contributing to the gCSC-mediated M2 polarization of the MΦs. We found that physiological doses of human recombinant MIC-1 were able to inhibit phagocytosis and upregulate IL-10 and TGF- $\beta 1$ . However, MIC-1 did not markedly increase p-STAT3 in MΦs, down modulate the costimulatory molecules (data not shown) or induce the MΦ's ability to inhibit T-cell proliferation (data not shown).

Furthermore, although physiological doses of MIC-1 did induce IL-10 and TGF- $\beta$ , these were less than the amounts that were achieved with supernatants from the gCSCs, indicating that MIC-1 is not the sole contributor for M2 polarization. This indicates that there is a complex interplay between the gCSCs and the M $\Phi$  that involves both STAT3-dependent and -independent processes. Unfortunately, because there is no commercially available antibody that will specifically block human MIC-1, we were not able to ascertain the relative contribution of MIC-1 and other gCSC-secreted products controlling the M2 polarization.

On the basis of the cumulative data, we present the following schema: the gCSC is elaborating CSF-1 that recruits the monocyte into the tumor microenvironment. Then, a variety of gCSC-secreted products, including MIC-1, induce the polarization of the monocytes to the immunosuppressive (M2) M $\Phi$ . Upon polarization to the M2 phenotype, the M $\Phi$  then acts in a protumorigenic manner by enhancing invasiveness, increasing tumor angiogenesis, and potentiating tumor-mediated immunosuppression by a variety of secreted products such as IL-10, TGF- $\beta$ , and IL-23, which would decrease Th1 skewing, decrease T-cell proliferation, and enhance Treg proliferation and recruitment (Fig. 4).

Another limitation and concern with an analysis of gCSCs maintained in vitro is the fact that we have noted the immunological changes in these cells over

time in culture. In order to negate this as much as possible, upon the initial isolation and characterization of these cells, we banked bulk gCSC-conditioned medium and used early passaged cells, but we have noted that with sequential passages the gCSCs become less immunosuppressive. Thus, our findings may underestimate the degree of gCSC-mediated immunosuppression that is exerted in vivo. Glioma cell lines that have lost their immunosuppressive capabilities over time may fail to recapitulate the level of immune suppression of de novo glioblastoma when used in animal models, and their response to immunotherapy may therefore not be reflective of the intrinsic in vivo biology. Thus, it will be essential for future research to delineate what factors of the native tumor microenvironment in which gCSCs are found, such as tissue hypoxia, are responsible for promoting and maintaining the immune suppressive phenotypes of these cells in vivo, and how they might be subject to therapeutic manipulation with agents such as hypoxia inducible factor-1 $\alpha$  inhibitors.

In this current study, we saw paradoxical increases in IL-10 and IL-23 using control siRNA that may be secondary to the engagement of toll-like receptors (TLRs) expressed on the gCSCs. Typically, TLR agonists on monocytes and M $\Phi$ s would result in their subsequent activation and proinflammatory function; however, TLR agonists can further attenuate immune suppression after M2 polarization.<sup>56,61-65</sup> It is therefore possible

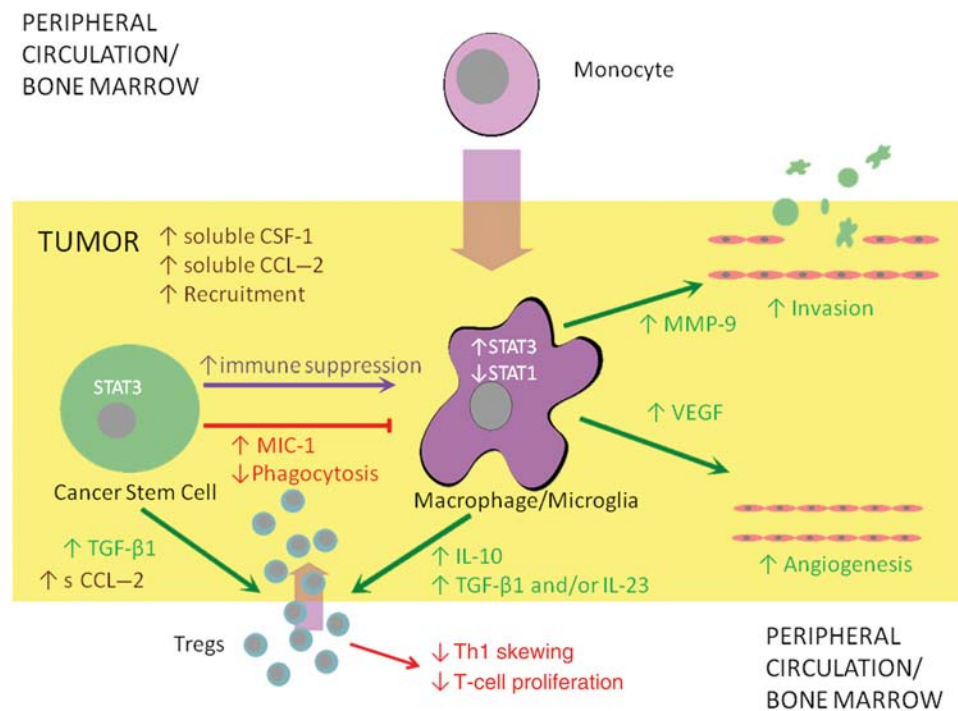


Fig. 4. Theoretical schema showing relationship between gCSCs and M $\Phi$ s. The gCSCs recruit circulating monocytes and Tregs via CSF-1 and CCL2 respectively and mediate differentiation and polarization of the monocytes into M2 tumor-associated M $\Phi$ s in part by elaboration of soluble MIC-1, increasing expression of p-STAT3 and decreasing expression of p-STAT1 in the monocytes/M $\Phi$ s. M2 tumor-associated M $\Phi$ s possess an immunosuppressive phenotype characterized by reduced phagocytosis, production of immunosuppressive cytokines including IL-10, TGF- $\beta$ 1, and/or IL-23, and the ability to inhibit T-cell proliferation. M2 tumor-associated M $\Phi$ s also contribute to other tumor-supportive functions, including angiogenesis and tissue remodeling allowing for invasion. The gCSCs also directly inhibit adaptive immunity by inducing Tregs. These immunosuppressive functions of gCSCs are mediated in part by STAT3.

that TLR agonists may actually potentiate gCSC-mediated immune suppression and is also an area of future investigation.

In addition to the gCSCs, another target cell that may be considered for therapeutic manipulation would be the immune suppressive M $\Phi$ /microglia, or its precursors, in order to counteract their tumor supportive activities with respect to immune suppression,<sup>13</sup> invasion,<sup>17</sup> and angiogenesis.<sup>10</sup> Therapeutic approaches could include inhibiting the polarization of the infiltrating M $\Phi$  to the M2 phenotype or the ability of either the M $\Phi$  or its circulating and bone marrow precursors to respond to gCSC signals, such that upon entry into the tumor microenvironment, these M $\Phi$ s do not become polarized toward the M2 immune suppressive and tumor supportive phenotype and instead toward the M1 phenotype that has antitumor activity. In order to ascertain the feasibility of this approach, it will be necessary to define the pathways in the M $\Phi$ s that are activated in response to gCSC signals.

The multimodal nature of glioblastoma-mediated immunosuppression has thwarted past attempts to treat this cancer with immunotherapy, wherein modulating any one or even several immune pathways proves ineffective because global immune suppression continues to be maintained by other redundant mechanisms. Because of the central role of gCSCs in glioblastoma initiation, progression, recurrence, resistance to chemotherapy and radiation, and immune suppression, the gCSC as an immune therapeutic target has recently garnered interest.<sup>66–68</sup> The potential for success for such strategies will depend on whether the self-protective immunosuppressive properties of gCSCs can be overcome such that these cells become exposed to immune recognition and vulnerable to immune clearance.<sup>69</sup> In this report, we demonstrate that the treatment of gCSCs with STAT3 siRNA or WP1066 restored phagocytosis and that the gCSC-exposed M $\Phi$ s were less inhibitory of adaptive immunity. Targeting the p-STAT3 pathway in the gCSCs represents a feasible therapeutic approach for the development of future novel therapies in the treatment of glioblastoma; however, this may not completely block the immunosuppressive functions of these cells, and other pathways are

likely to be contributing to the gCSC-mediated immunosuppression. p-STAT3 blockade may be used alone (promoting the host immune system's own capacity for tumor clearance) or in combination with other modes of immunotherapy, and we have recently shown that p-STAT3 blockade enhanced IFN- $\alpha$  immunotherapy in a murine metastatic melanoma model.<sup>70</sup> Similar synergistic therapeutic combinations may hold promise for glioblastoma as well. However, even p-STAT3 does not appear to be the whole story in gCSC-mediated immune suppression, and it appears that p-STAT3 independent mechanisms of immune suppression also exist in parallel. For example, in this study, we observed that MIC-1-mediated suppression of M $\Phi$ s did not appear to be wholly related to p-STAT3 activation. Therefore, it will be necessary to identify and characterize other major transcriptional hubs like p-STAT3 that play roles in the mediation of multiple downstream immune modulatory pathways in order to appropriately formulate therapeutic immune strategies.

## Supplementary material

Supplementary material is available at *Neuro-Oncology Journal* online.

## Acknowledgments

We thank Lamonne Crutcher for assistance in obtaining tissue specimens and David M. Wildrick, PhD, for editorial assistance.

*Conflict of interest statement.* W.P. and A.B.H. hold patents on WP1066.

## Funding

This work was supported by the Mitchell Foundation, the Dr Marnie Rose Foundation, The University of Texas MD Anderson Cancer Center, and the US National Institute of Health (CA120813-04).

## References

1. Streit WJ, Kreutzberg GW. Response of endogenous glial cells to motor neuron degeneration induced by toxic ricin. *J Comp Neurol.* 1988;268:248–263.
2. Kostianovsky AM, Maier LM, Anderson RC, Bruce JN, Anderson DE. Astrocytic regulation of human monocytic/microglial activation. *J Immunol.* 2008;181:5425–5432.
3. van Rossum D, Hanisch UK. Microglia. *Metab Brain Dis.* 2004;19:393–411.
4. Brault MS, Kurt RA. Impact of tumor-derived CCL2 on macrophage effector function. *J Biomed Biotechnol.* 2005;2005:37–43.
5. Conti I, Rollins BJ. CCL2 (monocyte chemoattractant protein-1) and cancer. *Semin Cancer Biol.* 2004;14:149–154.
6. Lamagna C, Aurrand-Lions M, Imhof BA. Dual role of macrophages in tumor growth and angiogenesis. *J Leukoc Biol.* 2006;80:705–713.
7. Pixley FJ, Stanley ER. CSF-1 regulation of the wandering macrophage: complexity in action. *Trends Cell Biol.* 2004;14:628–638.
8. Lin EY, Nguyen AV, Russell RG, Pollard JW. Colony-stimulating factor 1 promotes progression of mammary tumors to malignancy. *J Exp Med.* 2001;193:727–740.
9. Mantovani A, Bottazzi B, Colotta F, Sozzani S, Ruco L. The origin and function of tumor-associated macrophages. *Immunol Today.* 1992;13:265–270.
10. Pollard JW. Tumour-educated macrophages promote tumour progression and metastasis. *Nat Rev Cancer.* 2004;4:71–78.

11. Elgert KD, Alleva DG, Mullins DW. Tumor-induced immune dysfunction: the macrophage connection. *J Leukoc Biol.* 1998;64:275–290.
12. Hussain SF, Yang D, Suki D, Aldape K, Grimm E, Heiberger AB. The role of human glioma-infiltrating microglia/macrophages in mediating antitumor immune responses. *Neurooncology.* 2006;8:261–279.
13. Hussain SF, Yang D, Suki D, Grimm E, Heiberger AB. Innate immune functions of microglia isolated from human glioma patients. *J Transl Med.* 2006;4:15.
14. Savage ND, de Boer T, Walburg KV, et al. Human anti-inflammatory macrophages induce Foxp3+ GITR+ CD25+ regulatory T cells, which suppress via membrane-bound TGFbeta-1. *J Immunol.* 2008;181:2220–2226.
15. Umemura N, Saio M, Suwa T, et al. Tumor-infiltrating myeloid-derived suppressor cells are pleiotropic-inflamed monocytes/macrophages that bear M1- and M2-type characteristics. *J Leukoc Biol.* 2008;83:1136–1144.
16. Mantovani A, Sica A, Allavena P, Garlanda C, Locati M. Tumor-associated macrophages and the related myeloid-derived suppressor cells as a paradigm of the diversity of macrophage activation. *Hum Immunol.* 2009;70:325–330.
17. Sliwa M, Markovic D, Gabrusiewicz K, et al. The invasion promoting effect of microglia on glioblastoma cells is inhibited by cyclosporin A. *Brain.* 2007;130:476–489.
18. Wesolowska A, Kwiatkowska A, Slomnicki L, et al. Microglia-derived TGF-beta as an important regulator of glioblastoma invasion—an inhibition of TGF-beta-dependent effects by shRNA against human TGF-beta type II receptor. *Oncogene.* 2008;27:918–930.
19. Voronov E, Shouval DS, Krelin Y, et al. IL-1 is required for tumor invasiveness and angiogenesis. *Proc Natl Acad Sci USA.* 2003;100:2645–2650.
20. Hiratsuka S, Nakamura K, Iwai S, et al. MMP9 induction by vascular endothelial growth factor receptor-1 is involved in lung-specific metastasis. *Cancer Cell.* 2002;2:289–300.
21. Bingle L, Brown NJ, Lewis CE. The role of tumour-associated macrophages in tumour progression: implications for new anticancer therapies. *J Pathol.* 2002;196:254–265.
22. Rodero M, Marie Y, Coudert M, et al. Polymorphism in the microglial cell-mobilizing CX3CR1 gene is associated with survival in patients with glioblastoma. *J Clin Oncol.* 2008;26:5957–5964.
23. Galli R, Binda E, Orfanelli U, et al. Isolation and characterization of tumorigenic, stem-like neural precursors from human glioblastoma. *Cancer Res.* 2004;64:7011–7021.
24. Sanai N, Alvarez-Buylla A, Berger MS. Neural stem cells and the origin of gliomas. *N Engl J Med.* 2005;353:811–822.
25. Wei J, Barr J, Kong L-Y, et al. Glioma associated cancer-initiating cells induce immune suppression. *Clin Cancer Res.* 2010;16:461–473.
26. Wei J, Bar J, Kong L-Y, et al. Glioblastoma cancer-initiating cells inhibit T cell proliferation and effector responses by the STAT3 pathway. *Mol Cancer Ther.* 2010;9:67–78.
27. Kortylewski M, Yu H. Role of Stat3 in suppressing anti-tumor immunity. *Curr Opin Immunol.* 2008;20:228–233.
28. Abou-Ghazal M, Yang DS, Qiao W, et al. The incidence, correlation with tumor-infiltrating inflammation, and prognosis of phosphorylated STAT3 expression in human gliomas. *Clin Cancer Res.* 2008;14:8228–8235.
29. Yu H, Jove R. The STATs of cancer—new molecular targets come of age. *Nat Rev Cancer.* 2004;4:97–105.
30. Yu H, Kortylewski M, Pardoll D. Crosstalk between cancer and immune cells: role of STAT3 in the tumour microenvironment. *Nat Rev Immunol.* 2007;7:41–51.
31. Kortylewski M, Kujawski M, Wang T, et al. Inhibiting Stat3 signaling in the hematopoietic system elicits multicomponent antitumor immunity. *Nat Med.* 2005;11:1314–1321.
32. Lang R, Patel D, Morris JJ, Rutschman RL, Murray PJ. Shaping gene expression in activated and resting primary macrophages by IL-10. *J Immunol.* 2002;169:2253–2263.
33. Matsukawa A, Kudo S, Maeda T, et al. Stat3 in resident macrophages as a repressor protein of inflammatory response. *J Immunol.* 2005;175:3354–3359.
34. O'Farrell AM, Liu Y, Moore KW, Mui AL. IL-10 inhibits macrophage activation and proliferation by distinct signaling mechanisms: evidence for Stat3-dependent and independent pathways. *EMBO J.* 1998;17:1006–1018.
35. Sherry MM, Reeves A, Wu JK, Cochran BH. STAT3 is required for proliferation and maintenance of multipotency in glioblastoma stem cells. *Stem Cells.* 2009;27:2383–2392.
36. Bootcov MR, Bauskin AR, Valenzuela SM, et al. MIC-1, a novel macrophage inhibitory cytokine, is a divergent member of the TGF-beta superfamily. *Proc Natl Acad Sci USA.* 1997;94:11514–11519.
37. Strelau J, Schmeer C, Peterziel H, et al. Expression and putative functions of GDF-15, a member of the TGF-beta superfamily, in human glioma and glioblastoma cell lines. *Cancer Lett.* 2008;270:30–39.
38. Shnaper S, Desbaillets I, Brown DA, et al. Elevated levels of MIC-1/GDF15 in the cerebrospinal fluid of patients are associated with glioblastoma and worse outcome. *Int J Cancer.* 2009;125:2624–2630.
39. Mildner A, Schmidt H, Nitsche M, et al. Microglia in the adult brain arise from Ly-6ChiCCR2+ monocytes only under defined host conditions. *Nat Neurosci.* 2007;10:1544–1553.
40. Hussain SF, Kong L-Y, Jordan J, et al. A novel small molecule inhibitor of signal transducers and activators of transcription 3 reverses immune tolerance in malignant glioma patients. *Cancer Res.* 2007;67:9630–9636.
41. Bao S, Wu Q, McLendon RE, et al. Glioma stem cells promote radioresistance by preferential activation of the DNA damage response. *Nature.* 2006;444:756–760.
42. Liu G, Yuan X, Zeng Z, et al. Analysis of gene expression and chemoresistance of CD133+ cancer stem cells in glioblastoma. *Mol Cancer.* 2006;5:67–79.
43. Sun Y, Kong W, Falk A, et al. CD133 (Prominin) negative human neural stem cells are clonogenic and tripotent. *PLoS One.* 2009;4:e5498.
44. Shmelkov SV, Butler JM, Hooper AT, et al. CD133 expression is not restricted to stem cells, and both CD133+ and CD133- metastatic colon cancer cells initiate tumors. *J Clin Invest.* 2008;118:2111–2120.
45. Bleau AM, Hambarzumyan D, Ozawa T, et al. PTEN/PI3K/Akt pathway regulates the side population phenotype and ABCG2 activity in glioma tumor stem-like cells. *Cell Stem Cell.* 2009;4:226–235.
46. Zhang P, Lathia JD, Flavahan WA, Rich JN, Mattson MP. Squelching glioblastoma stem cells by targeting REST for proteasomal degradation. *Trends Neurosci.* 2009;32:559–565.
47. Verreck FA, de Boer T, Langenberg DM, et al. Human IL-23-producing type 1 macrophages promote but IL-10-producing type 2 macrophages subvert immunity to (myco)bacteria. *Proc Natl Acad Sci USA.* 2004;101:4560–4565.
48. Badie B, Schartner J. Role of microglia in glioma biology. *Microsc Res Tech.* 2001;54:106–113.
49. Nardin A, Abastado JP. Macrophages and cancer. *Front Biosci.* 2008;13:3494–3505.

50. Ford AL, Goodsall AL, Hickey WF, Sedgwick JD. Normal adult ramified microglia separated from other central nervous system macrophages by flow cytometric sorting. Phenotypic differences defined and direct ex vivo antigen presentation to myelin basic protein-reactive CD4+ T cells compared. *J Immunol.* 1995;154:4309–4321.
51. Kruisbeek AM, Shevach E, Thornton AM. Proliferative assays for T cell function. *Curr Protoc Immunol.* 2004;3.12.11–13.12.20.
52. Mancino A, Lawrence T. Nuclear factor-kappaB and tumor-associated macrophages. *Clin Cancer Res.* 2010;16:784–789.
53. Maeda H, Kuwahara H, Ichimura Y, Ohtsuki M, Kurakata S, Shiraishi A. TGF-beta enhances macrophage ability to produce IL-10 in normal and tumor-bearing mice. *J Immunol.* 1995;155:4926–4932.
54. Langowski JL, Kastelein RA, Oft M. Swords into plowshares: IL-23 repurposes tumor immune surveillance. *Trends Immunol.* 2007;28:207–212.
55. Leidi M, Gotti E, Bologna L, et al. M2 macrophages phagocytose rituximab-opsonized leukemic targets more efficiently than m1 cells in vitro. *J Immunol.* 2009;182:4415–4422.
56. Martinez FO, Sica A, Mantovani A, Locati M. Macrophage activation and polarization. *Front Biosci.* 2008;13:453–461.
57. Crane CA, Han SJ, Barry JJ, Ahn BJ, Lanier LL, Parsa AT. TGF-beta downregulates the activating receptor NKG2D on NK cells and CD8+ T cells in glioma patients. *Neurooncology.* 2010;12:7–13.
58. Biollaz G, Bernasconi L, Cretton C, et al. Site-specific anti-tumor immunity: differences in DC function, TGF-beta production and numbers of intratumoral Foxp3+ Treg. *Eur J Immunol.* 2009;39:1323–1333.
59. Sharma S, Stolina M, Luo J, et al. Secondary lymphoid tissue chemokine mediates T cell-dependent antitumor responses in vivo. *J Immunol.* 2000;164:4558–4563.
60. Johnen H, Lin S, Kuffner T, et al. Tumor-induced anorexia and weight loss are mediated by the TGF-beta superfamily cytokine MIC-1. *Nat Med.* 2007;13:1333–1340.
61. Hu X, Chen J, Wang L, Ivashkiv LB. Crosstalk among Jak-STAT, Toll-like receptor, and ITAM-dependent pathways in macrophage activation. *J Leukoc Biol.* 2007;82:237–243.
62. Kortylewski M, Kujawski M, Herrmann A, et al. Toll-like receptor 9 activation of signal transducer and activator of transcription 3 constrains its agonist-based immunotherapy. *Cancer Res.* 2009;69:2497–2505.
63. Opitz CA, Litzemberger UM, Lutz C, et al. Toll-like receptor engagement enhances the immunosuppressive properties of human bone marrow-derived mesenchymal stem cells by inducing indoleamine-2,3-dioxygenase-1 via interferon-beta and protein kinase R. *Stem Cells.* 2009;27:909–919.
64. Porta C, Rimoldi M, Raes G, et al. Tolerance and M2 (alternative) macrophage polarization are related processes orchestrated by p50 nuclear factor kappaB. *Proc Natl Acad Sci USA.* 2009;106:14978–14983.
65. Zhang Y, Woodruff M, Miao J, et al. Toll-like receptor 4 mediates chronic restraint stress-induced immune suppression. *J Neuroimmunol.* 2008;194:115–122.
66. Brown CE, Starr R, Martinez C, et al. Recognition and killing of brain tumor stem-like initiating cells by CD8+ cytolytic T cells. *Cancer Res.* 2009;69:8886–8893.
67. Pellegatta S, Poliani PL, Corno D, et al. Neurospheres enriched in cancer stem-like cells are highly effective in eliciting a dendritic cell-mediated immune response against malignant gliomas. *Cancer Res.* 2006;66:10247–10252.
68. Xu Q, Liu G, Yuan X, et al. Antigen-specific T-cell response from dendritic cell vaccination using cancer stem-like cell-associated antigens. *Stem Cells.* 2009;27:1734–1740.
69. Hatiboglu AM, Wei J, Wu A, Heimberger AB. Immune therapeutic targeting of glioma cancer stem cells. *Targeted Oncology.* In Press.
70. Kong LY, Gelbard A, Wei J, et al. Inhibition of p-STAT3 enhances IFN-β efficacy against metastatic melanoma. *Clin Cancer Res.* 2010;16:2550–2561.